AMERICAN SOCIETY FOR MICROBIOLOGY | Journal of Virology®

GENE DELIVERY

In Vivo Live Imaging of Oncolytic Mammalian Orthoreovirus Expressing NanoLuc Luciferase in Tumor Xenograft Mice

Yuta Kanai,[a] Takahiro Kawagishi,[a] Yoshiharu Matsuura,[b] Takeshi Kobayashi[a]

[a]Department of Virology, Research Institute for Microbial Diseases, Osaka University, Osaka, Japan
[b]Department of Molecular Virology, Research Institute for Microbial Diseases, Osaka University, Osaka, Japan

ABSTRACT Wild-type mammalian reoviruses (MRVs) have been evaluated as oncolytic agents against various cancers; however, genetic modification methods for improving MRV agents have not been exploited fully. In the present study, using MRV strain T1L, we generated a reporter MRV that expresses a NanoLuc luciferase (NLuc) gene and used it for noninvasive imaging of MRV infection in tumor xenograft mice. NLuc and a P2A self-cleaving peptide gene cassette were placed upstream of the L1 gene open reading frame to enable bicistronic expression of NLuc and the L1 gene product. BALB/c nude mice intranasally infected with MRV expressing NLuc (rsT1L-NLuc) displayed bioluminescent signals in the chest area at 4 days postinfection (dpi), which is consistent with natural MRV infection in the lung. Furthermore, to monitor tumor-selective infection by MRV, nude mice bearing human cancer xenografts were infected intravenously with rsT1L-NLuc. Bioluminescent signals were detected in tumors as early as 3 dpi and persisted for 2 months. The results demonstrate the utility of an autonomous replicating reporter MRV for noninvasive live imaging of replicating oncolytic MRV agents.

IMPORTANCE Engineering of recombinant MRV for improved oncolytic activity has not yet been achieved due to difficulty in generating autonomous replicating MRV harboring transgenes. Here, we constructed a reporter MRV that can be used to monitor cancer-selective infection by oncolytic MRV in a mouse model. Among the numerous oncolytic viruses, MRV has an advantage in that the wild-type virus shows marked oncolytic activity in patients without any notable adverse effects. The reporter MRV developed herein will open avenues to the development of recombinant MRV vectors armed with anticancer transgenes.

KEYWORDS cancer treatment, mammalian orthoreovirus, oncolytic virus, reporter virus

Oncolytic viral therapies based on naturally occurring or engineered oncolytic viruses that replicate selectively and trigger oncolysis have been developed over many years (1, 2). Mammalian orthoreoviruses (MRVs), which belong to the family *Reoviridae*, are common human pathogens that have oncolytic potential (3–5). MRV infections generally cause mild or asymptomatic infections, although certain case reports have indicated minor respiratory and gastrointestinal tract symptoms or the involvement of the central nervous system (6–8). A clone of MRV serotype T3D (called Reolysin; Oncolytics Biotech, Inc.), which has marked oncolytic activity, has been tested in clinical trials against various cancers (9–11). However, development of engineered MRV agents has been delayed due to difficulties in generating gene-modified MRV. A complete reverse genetics system for MRV opened up avenues for generating recombinant MRV to improve oncolytic activity (12); however, progress has been slow.

Monitoring dissemination of an oncolytic agent is important for noninvasive evaluation of the efficacy of delivery, as well as toxicity. Various types of reporter virus

Citation Kanai Y, Kawagishi T, Matsuura Y, Kobayashi T. 2019. *In vivo* live imaging of oncolytic mammalian orthoreovirus expressing NanoLuc luciferase in tumor xenograft mice. J Virol 93:e00401-19. https://doi.org/10.1128/JVI.00401-19.

Editor Susana López, Instituto de Biotecnologia/UNAM

Address correspondence to Takeshi Kobayashi, tkobayashi@biken.osaka-u.ac.jp.

Received 8 March 2019
Accepted 18 April 2019
Accepted manuscript posted online 8 May 2019
Published 28 June 2019

expressing luciferase genes have been tested to enable live imaging of viral replication and dissemination *in vivo* (13–15). Prototype reporter MRVs harboring a chloramphenicol acetyltransferase gene inserted into the MRV S2 gene segment, or a green fluorescent protein gene inserted into the S4 gene segment, replicate only in permissive cell lines expressing S2 or S4 gene products, respectively (12, 16). Autonomous replicating MRVs harboring iLOV or UnaG fluorescent genes in the S1 gene segment lack expression of an intact σ1 capsid protein, which affects MRV infectivity (17, 18). Use of these reporter MRVs for oncolytic research is restricted due to a lack of essential viral proteins. Recently, a novel strategy for developing an MRV transduction vector using a viral 2A-like element that enables bicistronic expression of a transgene without compromising expression of viral genes was developed (19). This robust technique using a 2A-like element is capable of inserting any transgene into a viral gene and so has potential for development of improved MRV oncolytic agents.

Here, as the primary step in the development of an engineered MRV oncolytic agent, we used a porcine teschovirus-1 2A (P2A) self-cleaving peptide to develop an autonomously replicating reporter MRV expressing NanoLuc luciferase (NLuc). NLuc activity in virus-infected cells correlated with viral infectious titers. *In vivo* live imaging of tumor-bearing mice infected with reporter MRV enabled monitoring of the time course of tumor-specific infection for up to 2 months postinfection.

RESULTS

Generation of NLuc expressing reporter MRV strain T1L. To generate autonomously replicating recombinant MRV strain T1L expressing a reporter gene, the NLuc-P2A peptide gene cassette was inserted between nucleotides 124 and 125 of the T1L L1 gene encoding the λ3 protein (Fig. 1A) by following the strategy described previously (19). The P2A peptide is a self-cleaving peptide that enables bicistronic translation of two open reading frames (ORFs) upstream and downstream of the P2A peptide (20). Disruption of the λ3 ORF by insertion of the NLuc-P2A cassette was reconstituted by duplication of the N-terminal region (nucleotides 19 to 124) of the L1 gene (Fig. 1A). L929 cells expressing T7 RNA polymerase were cotransfected with rescue plasmid pT7-L1-NLuc-P2A and nine other segment cDNAs from MRV T1L, and a recombinant strain of MRV T1L expressing NLuc (rsT1L-NLuc) was rescued. Wild-type recombinant strain T1L (rsT1L), generated by reverse genetics, was used as a control. Electrophoresis of the double-stranded RNA (dsRNA) genome revealed that rsT1L-NLuc possessed a larger L1 gene segment than wild-type rsT1L (Fig. 1B). Although the replication kinetics of rsT1L-NLuc were slightly lower than those of rsT1L (Fig. 1C), cell lysates derived from rsT1L-NLuc-infected cells showed increased NLuc activity over the time course of infection, indicating that the foreign NLuc gene in rsT1L-NLuc was stable (Fig. 1D). Next, we examined the correlation between virus titers and NLuc activity in cell lysates derived from various human cancer cell lines. We found that rsT1L-NLuc replication differed in eight human cancer cell lines (Fig. 1E) and that NLuc activity in cell lysates correlated with the virus infectious titer (Fig. 1F and G). Thus, both growth and NLuc activity of rsT1L-NLuc were sufficiently robust to enable *in vitro* examination of MRV.

Live imaging of virus replication in mice. A previous study showed that intranasal infection of adult BALB/c mice with MRV strain T1L leads to robust viral replication in the lung and subsequent spread to peripheral organs (21). Therefore, to evaluate the dynamics of viral infection in mice, we intranasally infected adult nude mice (BALB/cAJcl-nu) with either rsT1L or rsT1L-NLuc. At 2 days postinfection (dpi), a bioluminescence signal was observed in the chest of rsT1L-NLuc-infected mice (Fig. 2A). To identify the organs expressing the bioluminescence signal, animals were sacrificed at 4 dpi and internal organs were exposed. In the open body cavity, bioluminescence signals were restricted to the lungs (Fig. 2B). The luminescence signal in the lungs intensified at 4 and 6 dpi. At 6 dpi, we detected luminescence signals in the abdominal region. To examine the correlation between bioluminescence signals and virus replication, infected mice were sacrificed, and the infectious virus titer in the organs was examined (Fig. 2C and D). At 2 and 4 dpi, infectious viruses were detected preferentially in the

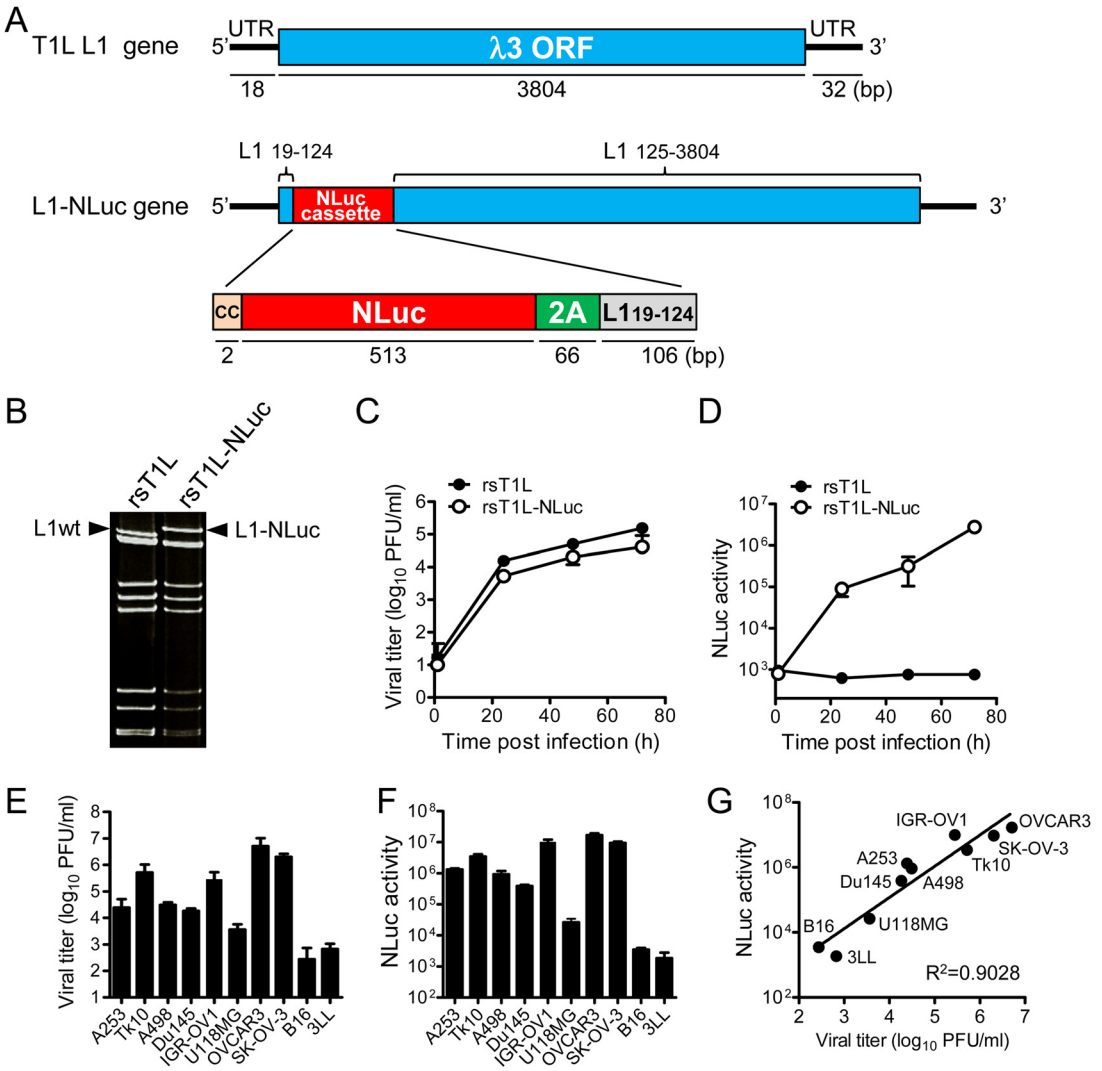

FIG 1 Generation of reporter MRV. (A) Schematic showing generation of rsT1L-NLuc using an MRV reverse genetics system. The NLuc-P2A cassette was inserted into the L1 gene between nucleotides 124 and 125. To express NLuc-P2A as a fusion peptide with the L1 ORF N-terminal region, additional CC nucleotides were inserted before the NLuc-P2A cassette. The region comprising nucleotides 19 to 124 of the L1 gene was duplicated after the NLuc-P2A cassette to reconstruct the L1 ORF. (B) Electrophoresis of dsRNA purified from rsT1L and rsT1L-NLuc. Arrowheads indicate the L1wt and L1-NLuc gene segments. (C and D) Kinetics of virus replication and NLuc activity of rsT1L-NLuc in L929 cells. (E to G) Correlation between viral replication and NLuc activity of rsT1L-NLuc in human and murine cancer cell lines. Cells were infected with rsT1L-NLuc at an MOI of 0.01 PFU/cell and incubated for 48 h. Viral infectious titers and NLuc activity in the cell lysates were then determined.

lungs. At 6 dpi, viruses were also detected in the intestine (consistent with the bioluminescence images). Although both rsT1L and rsT1L-NLuc exhibited similar time courses of viral dissemination, the viral titers of rsT1L-NLuc in each organ was lower than those of rsT1L. These results indicate that bioluminescence images from rsT1L-NLuc-infected mice reflect the real-time dynamics of lung infection.

Noninvasive, real-time imaging of selective infection of tumors by MRV after intravenous injection. MRV selectively infects and replicates in tumors after intravenous or intraperitoneal injection (22, 23). Therefore, to examine the utility of rsT1L-NLuc for tracking virus replication in mice bearing human cancer xenografts, BALB/c nude mice were implanted subcutaneously with epidermoid carcinoma A253 cells (Fig. 3A to C) or ovarian cancer IGR-OV1 cells (Fig. 3D to F). When implanted cancer cells formed tumors measuring approximately 5 mm in diameter, rsT1L or rsT1L-NLuc was injected intravenously via the tail vein. At 7 dpi, tumor-specific bioluminescence images were obtained only in rsT1L-NLuc-infected mice bearing A253 or IGR-OV1 cancer cell xeno-

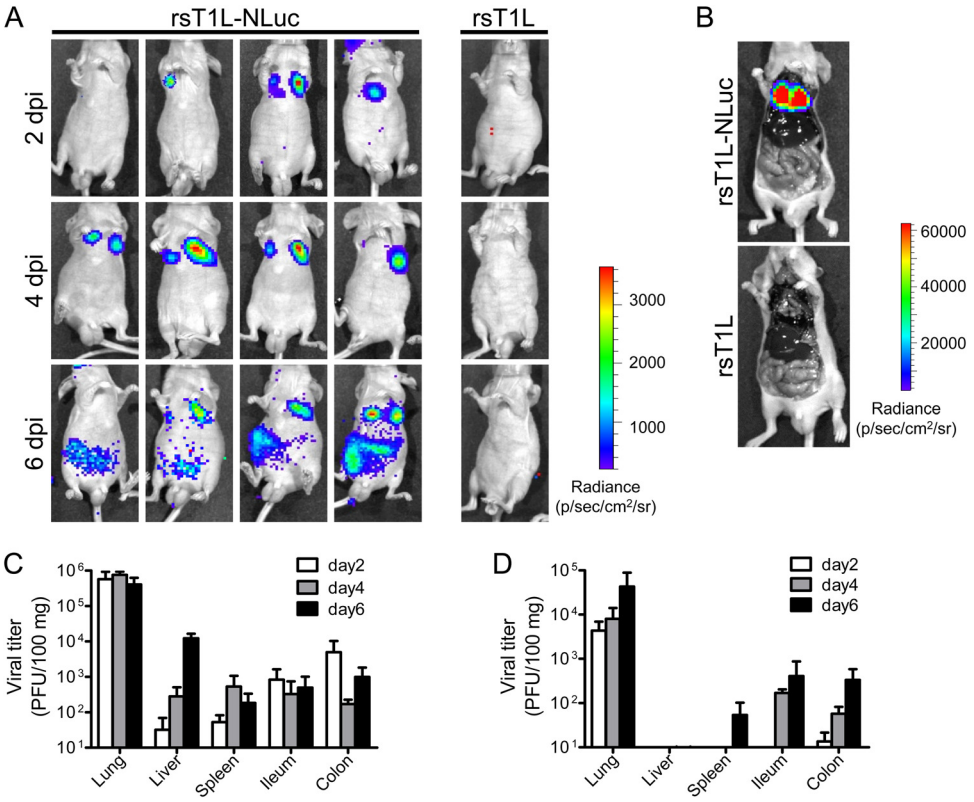

FIG 2 Live luminescence imaging of rsT1L-NLuc virus infection in mice. (A to D) BALB/c nude mice were infected intranasally with 1.4×10^7 PFU of rsT1L or rsT1L-NLuc. At 2, 4, or 6 days postinfection (dpi), NLuc substrates were injected via the retro-orbital venous sinus and the bioluminescence signal was obtained using an *in vivo* imaging system (IVIS). (B) At 4 dpi, animals were sacrificed after inoculation of NLuc substrate and the body cavities were opened. Carcasses were subjected to IVIS observation. (C and D) At 2, 4, or 6 dpi, animals were sacrificed after IVIS observation and infectious virus titers in tissue homogenates were examined. (C) rsT1L; (D) rsT1L-NLuc. Data are expressed as the mean ± standard deviation (SD) ($n = 4$).

grafts (Fig. 3A and D). To evaluate the association between the bioluminescence signal and virus replication, the infectious virus titers and NLuc activities in tissue homogenates were examined. In both A253 and IGR-OV1 xenograft mice, the highest viral titers and NLuc activities were found in tumor homogenates, followed by lung tissue (Fig. 3B, C, E, and F). Although the viral titers and NLuc activities were correlated in rsT1L-NLuc-infected mice, no positive NLuc activities were detected in rsT1L-infected mice. These results demonstrate that rsT1L-NLuc is useful for tracking tumor-selective infection by MRV.

Long-term tracking of MRV infection in mice bearing human cancer xenografts. Finally, we conducted long-term observations of cancer-selective infection by rsT1L-NLuc virus. BALB/c nude mice were implanted subcutaneously with prostate cancer Du145 cells. At 14 dpi, mice were injected intravenously with either rsT1L or rsT1L-NLuc via the tail vein. Tumor-specific luminescence signals were observed as early as 3 dpi in rsT1L-NLuc-infected mice. The bioluminescence signal persisted for up to 60 dpi but disappeared by 80 dpi (Fig. 4A). Furthermore, we examined viral titers and NLuc activity in mice infected with either rsT1L or rsT1L-NLuc viruses at various time points postinfection (Fig. 4B to E). Infectious virus titers in organs from mice sacrificed on days 3, 6, 10, 33, and 80 postinfection revealed the largest amounts of rsT1L and rsT1L-NLuc viruses in tumors, followed by the lung, throughout the observation period (Fig. 4B and D). The highest NLuc activity at various time points postinfection was observed in xenograft tumors in mice infected with rsT1L-NLuc virus (Fig. 4C and E). We noticed that tumors continued to develop throughout the experiment, despite persistent infection by MRV. *In vitro* studies suggest that strain T1L shows mild to strong oncolytic activity

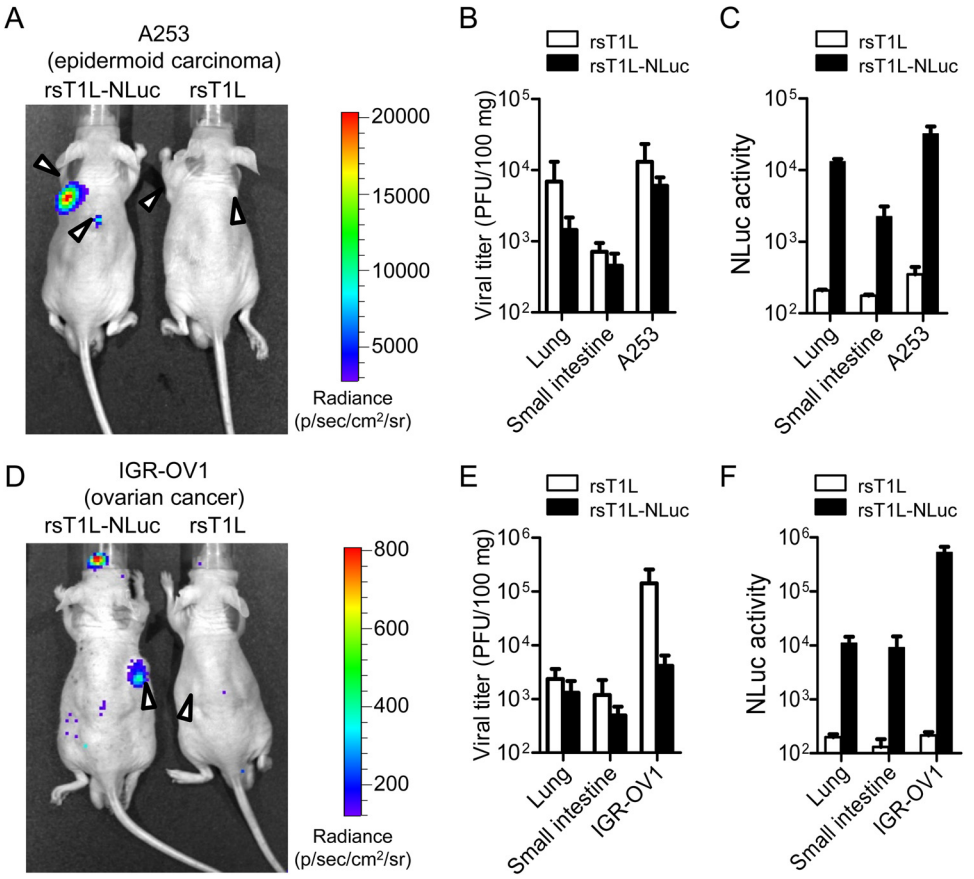

FIG 3 Bioluminescence imaging of MRV infection in human cancer xenografts. BALB/c nude mice transplanted with human cancer cell lines A253 (A to C) or IGR-OV1 (D to F) were infected intravenously with 7.0×10^7 PFU of rsT1L or rsT1L-NLuc. At 7 days postinfection, animals were injected with NLuc substrate via the retro-orbital venous sinus and bioluminescence images were obtained using an IVIS. Arrowheads indicate tumors. After observation, the animals were sacrificed and viral titers (B and E) and NLuc activity (C and F) in the lungs, small intestine, and tumors were examined. Data are expressed as the mean ± SD ($n = 3$).

in cancer cells, depending on the cell type (24). Therefore, we examined the oncolytic activity of rsT1L in Du145 cells. Consistent with the *in vivo* experiments, we found that rsT1L demonstrated only weak cell killing activity against Du145 cells *in vitro* (Fig. 4F). These results suggest that rsT1L-NLuc is a useful tool for studying MRV replication and spread over long periods of time.

DISCUSSION

In 2015, the first oncolytic viral therapy, T-VEC, an oncolytic herpes simplex virus 1 (HSV-1) expressing granulocyte macrophage colony-stimulating factor (GM-CSF) was approved in the the United States for treatment of advanced malignant melanoma (25, 26). The success of T-VEC will accelerate the development of oncolytic viral therapy using different oncolytic viral agents. Although Reolysin, a clone of the wild-type MRV T3D strain, has been around for a long time, difficulties with gene modification have led to a bottleneck to further development of engineered MRV agents. Here, we used a bicistronic expression system based on a P2A peptide to develop an autonomous replicating reporter MRV T1L strain.

When an RNA virus is being engineered for use as a viral transduction vector, a major problem is the instability of the transgene. To reduce the effects of insertion of a foreign gene, we used an NLuc expression system, because it is smaller and has higher sensitivity than other luciferase genes. For example, the NLuc gene (0.5 kbp) in an engineered reporter Sindbis virus is more stable than the firefly luciferase gene (1.6 kbp) after serial passages (15). NLuc is a small, bright luciferase suitable for *in vivo*

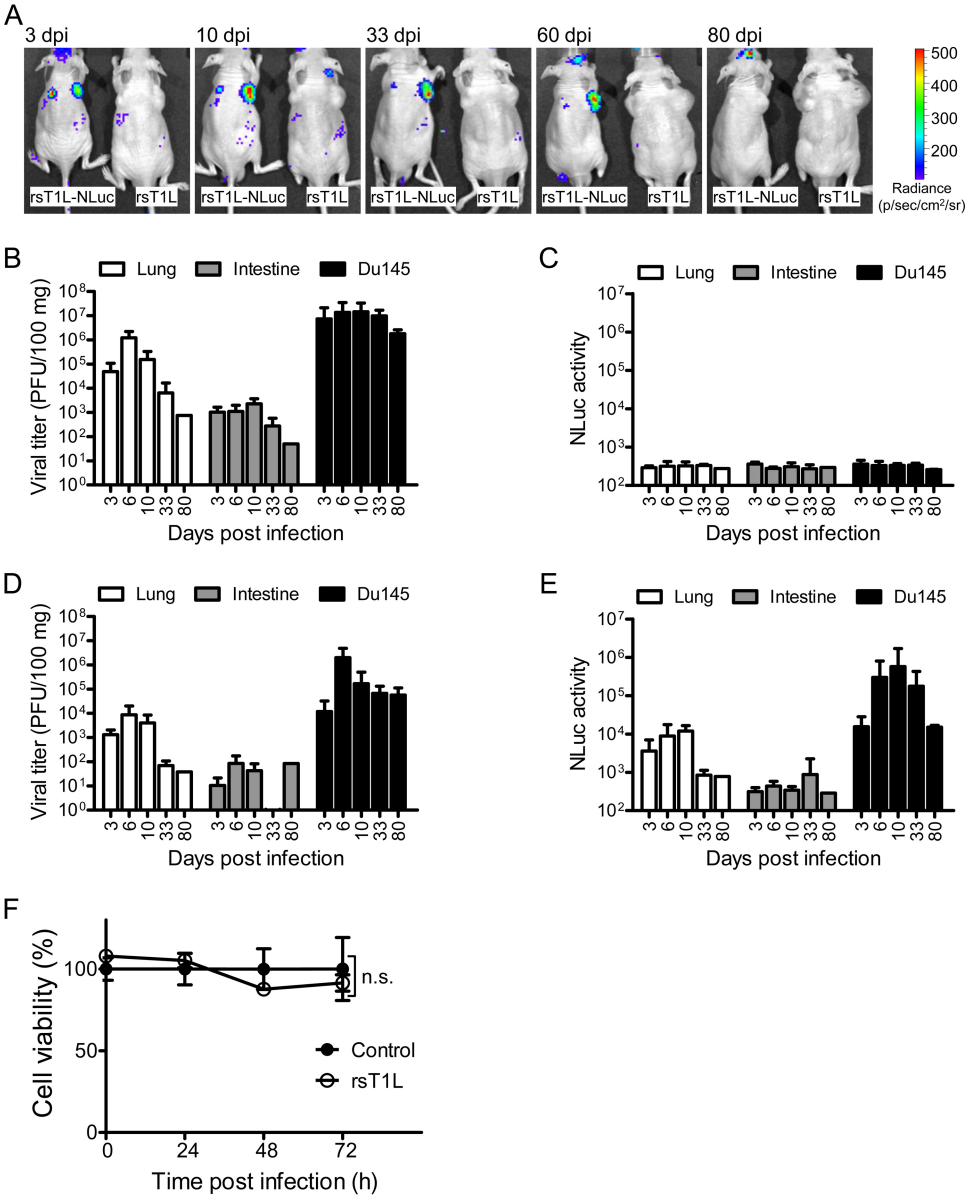

FIG 4 Bioluminescence imaging of rsT1L-NLuc infection of human cancer xenografts. BALB/c nude mice ($n = 15$ per group) implanted with human prostate cancer Du145 cells were infected intravenously with 7.0×10^7 PFU of rsT1L or rsT1L-NLuc. (A) At the indicated days postinfection, animals were injected with substrate via the orbital venous sinus. Bioluminescence images were obtained using an IVIS. Representative animals are shown. (B to E) After observation of bioluminescence signals via an IVIS, animals were sacrificed and virus titers (rsT1L [B] and rsT1L-NLuc [D]) and NLuc activity (rsT1L [C] and rsT1L-NLuc [E]) in the lungs, small intestine, and tumors were examined. Data are expressed as the mean ± SD ($n = 4$ at days 3 and 6, $n = 3$ at days 10 and 33, and $n = 1$ at day 80). (F) Oncolytic activity of MRV T1L in Du145 human cancer cells. Cells were infected with virus at an MOI of 10 PFU/cell, and cell viability was determined in a WST-1 assay. Cell viability (%) with respect to the control sample is shown. Significant differences in cell viability at 72 h postinfection were determined by *t* test. n.s., not statistically significant.

imaging (15, 27–29). To exploit the advantages of the NLuc gene for studying tumor selectivity, we generated recombinant MRV expressing NLuc, thereby enabling bioluminescence imaging of MRV infection in live tumor-bearing mice.

However, the peak emission wavelength of NLuc (460 nm) is not suitable for imaging of deep tissue in living animals. Indeed, the sensitivity of the bioluminescence signal generated by NLuc is not sufficient to detect small amounts of rsT1L-NLuc *in vivo*. Therefore, to develop a better reporter MRV, further improvement of the stability and utility of different reporter genes for *in vivo* imaging is required.

Here, we used reporter MRV for noninvasive imaging of the dynamics of MRV after intranasal infection, although the replication efficiency of rsT1L-NLuc was lower than that of rsT1L in mice and *in vitro*. Under natural conditions, MRV strain T1L infects animals via the intranasal or oral routes. Once a host is infected with MRV via the intranasal route, MRV replicates within respiratory organs and then spreads to the intestine via the bloodstream (30, 31). Several small rodent models, including immunocompetent and immunocompromised mice and rats, have been used to study infection and dissemination of MRV after administration via the intranasal and oral routes (21, 32–34). Furthermore, SCID mice and nude mice bearing human cancer xenografts have been used to study the oncolytic activity of MRV (22, 35–37). Here, we used nude mice to observe infection of MRV via the intranasal route because the lack of hair facilitates detection of bioluminescence signals. A single injection of rsT1L or rsT1L-NLuc led to long-term persistent infection of the lung and tumors. It is likely that long-term infection is associated with the lack of T lymphocytes in nude mice. In SCID mice, which lack both B and T lymphocytes, long-term persistent infection over 90 days has been reported (32, 38). Preexisting neutralizing antibodies in patient blood is a significant concern during clinical application of oncolytic viruses, as such antibodies will hamper transmission. Seroepidemiological studies demonstrate that most adults are exposed to reovirus infection and develop specific antibodies before the age of 19 years (39, 40). Thus, comparing dissemination of rsT1L-NLuc in immunocompetent mice with that in immunodeficient mice is an important subject for further study.

The oncolytic activities of MRV T1L and T3D strains differ according to cancer cell type. Currently, a clone of the T3D strain has been developed as an oncolytic agent due to its marked oncolytic effects; however, the T1L strain induces more cell death than the T3D strain in large-cell carcinoma cell lines (24). Unfortunately, the T1L strain used in the present study did not kill Du145 cancer cells effectively. Indeed, the sizes of the tumors in nude mice infected with rsT1L and rsT1L-NLuc did not decrease throughout the experiment, although virus infection persisted. Because evaluation of the oncolytic activity of MRV is a major reason for developing reporter oncolytic viruses, future studies should focus on developing modified reporter MRV viruses with robust oncolytic activity.

The bicistronic expression system using P2A peptide is expected to arm MRV with foreign genes that enhance oncolytic activity, for example, cancer immunity-stimulating genes such as those encoding interleukin-12 and GM-CSF (41, 42). It should be noted that the bicistronic expression system enables the insertion of foreign genes into N- and C-terminal ORFs. To generate a more stable MRV transduction vector, extensive research is needed to identify more suitable sites for insertion of the transgene-2A cassette. Alternatively, repeat serial passage and selection of transgene-positive virus clones may be effective, as shown by previous work on the generation of a stable reporter influenza virus (43).

We demonstrated that rsT1L-NLuc is a valuable tool for developing an *in vitro* reporter assay, because NLuc activity in cell lysates correlated with viral infectious titer in various cell lines. Replication of rsT1L-NLuc was, however, weaker than that of rsT1L, suggesting that insertion of the NLuc gene might affect genome packaging or expression of the λ3 ORF in the L1 gene segment. We are attempting to generate other reporter MRVs expressing fluorescent proteins that will facilitate live monitoring of viral infection and dissemination. Meanwhile, the reporter MRV will be of great benefit not only for cancer treatment but also as a tool for studying the basic biology of MRVs.

MATERIALS AND METHODS

Cells and viruses. L929, a mouse fibroblast cell line, was grown in Dulbecco modified Eagle medium (DMEM) supplemented with 5% fetal calf serum (FCS). Human cancer cell lines A253, Tk10, A498, Du145, IGR-OV1, U118MG, OVCAR3, and SK-OV-3 were maintained in RPMI 1640 supplemented with 10% FCS and 2 mM L-glutamine. Murine cancer cell lines B16 and 3LL (kindly provided by Cell Resource Center for Biomedical Research, Tohoku University, Sendai, Japan) were grown in DMEM supplemented with 5% FCS. Recombinant strains of wild-type mammalian orthoreovirus type T1L (rsT1L) were recovered using a reverse genetics system (44). Virus infectious titers were determined in a plaque assay with L929 cells. In brief, viruses (diluted 10-fold) were inoculated onto a monolayer of L929 cells. After 1 h, culture

medium was removed and overlaid with 0.8% agarose gel. At 6 dpi, cells were overlaid with 0.8% agarose gel containing neutral red and incubated overnight, and plaque numbers were counted. Attenuated vaccinia virus strain rDls-T7pol expressing T7 RNA polymerase was propagated in chicken embryo fibroblasts (45).

Plasmid construction. MRV T1L rescue plasmids pT7-L1T1L, pT7-L2T1L, pT7-L3T1L, pT7-M1T1L, pT7-M2T1L, pT7-M3T1L, pBacT7-S1T1L, pT7-S2T1L, pT7-S3T1L, and pT7-S4T1L were prepared as described previously (12, 44). To create pT7-L1T1L-NLuc, which contains the NLuc gene (GenBank accession number KM359774), and the self-cleaving P2A peptide gene of porcine teschovirus-1 (GSGATNFSLLKQ AGDVEENPGP), the NLuc-P2A gene cassette was amplified and inserted between nucleotides 124 and 125 of the L1 gene. To express NLuc-P2A as a fusion peptide with the L1 ORF N-terminal region, additional nucleotides (CC) were inserted before the NLuc-P2A cassette. Partial L1 gene nucleotide sequences spanning positions 19 to 124 were duplicated after the NLuc-P2A cassette to reconstitute the λ3 ORF.

Recovery of rsT1L-NLuc virus. Both rsT1L and rsT1L-NLuc were rescued using a plasmid-based reverse genetics system, as described previously (12). In brief, monolayers of L929 cells seeded in 12-well plates (Corning) were infected with rDls-T7pol at a multiplicity of infection (MOI) of approximately 0.5 $TCID_{50}$ (50% tissue culture infective dose)/cell. At 1 h postinfection, cells were cotransfected with plasmids harboring the cloned reovirus genome using 2 μl of TransIT-LT1 transfection reagent (Mirus) per microgram of plasmid DNA. Each mixture comprised 0.25 μg of each T1L rescue plasmid (pT7-L1T1L, pT7-L2T1L, pT7-L3T1L, pT7-M1T1L, pT7-M2T1L, pT7-M3T1L, pBacT7-S1T1L, pT7-S2T1L, pT7-S3T1L, and pT7-S4T1L). To rescue rsT1L-NLuc, pT7-L1T1L-NLuc was used instead of pT7-L1T1L. After 5 days of incubation, recombinant virus was isolated from transfected cells by plaque purification on L929 cells (46).

Electrophoresis of viral dsRNA genomes. Viral dsRNAs were extracted from rsT1L and rsT1L-NLuc virions and mixed with an equal volume of 2× sample buffer (125 mM Tris-HCl [pH 6.8], 10% [vol/vol] 2-mercaptoethanol, 4% [wt/vol] SDS, and 10% [wt/vol] sucrose). The dsRNAs were separated on 8% (wt/vol) polyacrylamide gels (Atto) and visualized by ethidium bromide staining.

Replication and expression of NLuc derived from rsT1L-NLuc in human cells *in vitro*. Monolayers of L929, A253, Tk10, A498, Du145, OVCAR53, and SK-O-3 cells in 12-well plates were infected with rsT1L or rsT1L-NLuc at an MOI of 0.01 PFU/cell and incubated for various times. Cells were lysed by freeze-thawing. Viral infectious titers in cell lysates were determined in a plaque assay. To detect NLuc activity, 50 μl of cell lysate was mixed with 10 μl of lysis buffer, 0.1 μl of Nano-Glo substrate (Promega), and 50 μl of phosphate-buffered saline (PBS). After incubation at room temperature, NLuc activity was measured in a luminometer.

Experimental infection of animals and *in vivo* imaging. Four-week-old male nude mice (BALB/cAJcl-nu/nu) were purchased from Japan Clea. To monitor dissemination of rsT1L-NLuc after intranasal infection, mice (n = 12/group) were inoculated intranasally with 1.4×10^7 PFU/20 μl of rsT1L or rsT1L-NLuc. At 2, 4, and 6 dpi, four mice per group were anesthetized with isoflurane (Dainippon Sumitomo Pharma) and inoculated with 100 μl of Nano-Glo substrate (Promega; 1:50 dilution in PBS) via the retro-orbital venous sinus using a 27-gauge needle fitted with a 1-ml syringe. At 1 min postinjection of Nano-Glo, bioluminescence signals were detected using an *in vivo* imaging system (IVIS 100; Xenogen) and Living Image software (Xenogen). The image was obtained with an open filter, and the acquisition time was 60 s. After observation, animals were sacrificed and internal organs (lung, liver, spleen, ileum, and colon) were collected, weighed, and homogenized in DMEM supplemented with 5% FCS and penicillin/streptomycin by use of a bead homogenizer (BeadSmash 12; WakenBtech Co., Ltd.). Virus infectious titers in tissue homogenates were determined in a plaque assay. Next, to establish a human cancer xenograft model, 4-week-old male nude mice (BALB/cAJcl-nu/nu) were implanted subcutaneously (on the right, left, or both sides of the back) with 1×10^6 human cancer cells (A253, IGR-OV1, or Du145). When the tumors reached a diameter of approximately 5 mm, mice were randomly divided into two groups. A253 (n = 3/group)- and IGR-OV1 (n = 3/group)-implanted mice received 100 μl of rsT1L (7.0×10^7 PFU) or rsT1L-NLuc (7.0×10^7 PFU) via the tail vein (27-gauge needle fitted with a 1-ml syringe). At 7 dpi, 100 μl of Nano-Glo substrate (1:50 dilution in PBS) was injected via the retro-orbital venous sinus. At 1 min postinjection of Nano-Glo, bioluminescence signals were detected using an IVIS. Du145-implanted mice (n = 15/group) received 100 μl of rsT1L (7.0×10^7 PFU) or rsT1L-NLuc (7.0×10^7 PFU). At 3 dpi (n = 4), 6 dpi (n = 4), 10 dpi (n = 3), 33 dpi (n = 3), 60 dpi (n = 1), and 80 dpi (n = 1), mice received 100 μl of Nano-Glo substrate (1:50 dilution in PBS) via the retro-orbital venous sinus and bioluminescence signals were detected using an IVIS. The signal intensity was represented by the radiance unit of photons (p) /sec/cm^2/sr. After observation, animals were sacrificed and internal organs (lung, small intestine, and tumors) were collected, weighed, and homogenized. Virus infectious titers in the tissue homogenates were determined in a plaque assay.

Cytotoxicity assay. Monolayers of Du145 cells cultured in 96-well plates were infected with virus at an MOI of 10 PFU/cell and incubated for various times. At the indicated times, cell viability was determined in a WST-1 assay. In brief, 2 μl of cell proliferation reagent was added to the cell culture and incubated at 37°C for 1 h, and the optical density at 440 nm was measured in a microplate reader (PowerScan HT; DS Pharma Biomedical, Osaka, Japan).

Statistical analyses. Statistical analyses were performed using GraphPad Prism (v5.0). Cell viabilities at 72 h postinfection were compared between two groups using the two-tailed Student's t test. A P of <0.05 was considered statistically significant.

Ethics statement. The study was approved by the Animal Research Committee of the Research Institute for Microbial Diseases, Osaka University (approval number Bi-Dou-25-06-0). All experiments

were conducted in accordance with the guidelines for the care and use of laboratory animals of the Ministry of Education, Culture, Sports, Science and Technology, Japan.

ACKNOWLEDGMENTS

We thank Naoko Nagasawa and Misa Onishi for technical assistance. We also thank Toru Okamoto for providing human cancer cell lines and for technical assistance, Fuminori Sakurai for technical assistance, and Shinichi Yokota for providing U118MG cells.

This work was supported in part by grants-in-aid from the Research Program on JSPS KAKENHI (grant numbers JP16K19138, JP25860340, and JP26292149).

Author contributions were as follows: conceptualization and design, Y. Kanai and T. Kobayashi; development of methodology, Y. Kanai and T. Kobayashi; acquisition of data, Y. Kanai and T. Kawagishi; data analysis and interpretation, Y. Kanai, T. Kawagishi, Y. Matsuura, and T. Kobayashi; writing of the manuscript, Y. Kanai, T. Kawagishi, Y. Matsuura, and T. Kobayashi.

We have no conflicts of interest.

REFERENCES

1. Bommareddy PK, Shettigar M, Kaufman HL. 2018. Integrating oncolytic viruses in combination cancer immunotherapy. Nat Rev Immunol 18:498–513. https://doi.org/10.1038/s41577-018-0014-6. (Author Correction, 18:498, https://doi.org/10.1038/s41577-018-0031-5.)
2. Twumasi-Boateng K, Pettigrew JL, Kwok YYE, Bell JC, Nelson BH. 2018. Oncolytic viruses as engineering platforms for combination immunotherapy. Nat Rev Cancer 18:419–432. https://doi.org/10.1038/s41568-018-0019-2. (Publisher Correction, 18:526, https://doi.org/10.1038/s41568-018-0019-2.)
3. Coffey MC, Strong JE, Forsyth PA, Lee PW. 1998. Reovirus therapy of tumors with activated Ras pathway. Science 282:1332–1334. https://doi.org/10.1126/science.282.5392.1332.
4. Sabin AB. 1959. Reoviruses. A new group of respiratory and enteric viruses formerly classified as ECHO type 10 is described. Science 130:1387–1389. https://doi.org/10.1126/science.130.3386.1387.
5. Strong JE, Coffey MC, Tang D, Sabinin P, Lee PW. 1998. The molecular basis of viral oncolysis: usurpation of the Ras signaling pathway by reovirus. EMBO J 17:3351–3362. https://doi.org/10.1093/emboj/17.12.3351.
6. Jackson GG, Muldoon RL, Cooper GS. 1961. Reovirus type I as an etiologic agent of common cold. J Clin Invest 40:1051.
7. Rosen L, Evans HE, Spickard A. 1963. Reovirus infections in human volunteers. Am J Hyg 77:29–37. https://doi.org/10.1093/oxfordjournals.aje.a120293.
8. Tyler KL, Barton ES, Ibach ML, Robinson C, Campbell JA, O'Donnell SM, Valyi-Nagy T, Clarke P, Wetzel JD, Dermody TS. 2004. Isolation and molecular characterization of a novel type 3 reovirus from a child with meningitis. J Infect Dis 189:1664–1675. https://doi.org/10.1086/383129.
9. Galanis E, Markovic SN, Suman VJ, Nuovo GJ, Vile RG, Kottke TJ, Nevala WK, Thompson MA, Lewis JE, Rumilla KM, Roulstone V, Harrington K, Linette GP, Maples WJ, Coffey M, Zwiebel J, Kendra K. 2012. Phase II trial of intravenous administration of Reolysin((R)) (Reovirus Serotype-3-dearing Strain) in patients with metastatic melanoma. Mol Ther 20:1998–2003. https://doi.org/10.1038/mt.2012.146.
10. Noonan AM, Farren MR, Geyer SM, Huang Y, Tahiri S, Ahn D, Mikhail S, Ciombor KK, Pant S, Aparo S, Sexton J, Marshall JL, Mace TA, Wu CS, El-Rayes B, Timmers CD, Zwiebel J, Lesinski GB, Villalona-Calero MA, Bekaii-Saab TS. 2016. Randomized phase 2 trial of the oncolytic virus pelareorep (Reolysin) in upfront treatment of metastatic pancreatic adenocarcinoma. Mol Ther 24:1150–1158. https://doi.org/10.1038/mt.2016.66.
11. Stoeckel J, Hay JG. 2006. Drug evaluation: Reolysin–wild-type reovirus as a cancer therapeutic. Curr Opin Mol Ther 8:249–260.
12. Kobayashi T, Antar AA, Boehme KW, Danthi P, Eby EA, Guglielmi KM, Holm GH, Johnson EM, Maginnis MS, Naik S, Skelton WB, Wetzel JD, Wilson GJ, Chappell JD, Dermody TS. 2007. A plasmid-based reverse genetics system for animal double-stranded RNA viruses. Cell Host Microbe 1:147–157. https://doi.org/10.1016/j.chom.2007.03.003.
13. Manicassamy B, Manicassamy S, Belicha-Villanueva A, Pisanelli G, Pulendran B, Garcia-Sastre A. 2010. Analysis of in vivo dynamics of influenza virus infection in mice using a GFP reporter virus. Proc Natl Acad Sci U S A 107:11531–11536. https://doi.org/10.1073/pnas.0914994107.
14. Schoggins JW, Dorner M, Feulner M, Imanaka N, Murphy MY, Ploss A, Rice CM. 2012. Dengue reporter viruses reveal viral dynamics in interferon receptor-deficient mice and sensitivity to interferon effectors in vitro. Proc Natl Acad Sci U S A 109:14610–14615. https://doi.org/10.1073/pnas.1212379109.
15. Sun C, Gardner CL, Watson AM, Ryman KD, Klimstra WB. 2014. Stable, high-level expression of reporter proteins from improved alphavirus expression vectors to track replication and dissemination during encephalitic and arthritogenic disease. J Virol 88:2035–2046. https://doi.org/10.1128/JVI.02990-13.
16. Roner MR, Joklik WK. 2001. Reovirus reverse genetics: incorporation of the CAT gene into the reovirus genome. Proc Natl Acad Sci U S A 98:8036–8041. https://doi.org/10.1073/pnas.131203198.
17. Eaton HE, Kobayashi T, Dermody TS, Johnston RN, Jais PH, Shmulevitz M. 2017. African swine fever virus NP868R capping enzyme promotes reovirus rescue during reverse genetics by promoting reovirus protein expression, virion assembly, and RNA incorporation into infectious virions. J Virol 91:e02416-16. https://doi.org/10.1128/JVI.02416-16..
18. van den Wollenberg DJM, Dautzenberg IJC, Ros W, Lipińska AD, van den Hengel SK, Hoeben RC. 2015. Replicating reoviruses with a transgene replacing the codons for the head domain of the viral spike. Gene Ther 22:267–279. https://doi.org/10.1038/gt.2014.126.
19. Demidenko AA, Blattman JN, Blattman NN, Greenberg PD, Nibert ML. 2013. Engineering recombinant reoviruses with tandem repeats and a tetravirus 2A-like element for exogenous polypeptide expression. Proc Natl Acad Sci U S A 110:E1867–E1876. https://doi.org/10.1073/pnas.1220107110.
20. Kim JH, Lee SR, Li LH, Park HJ, Park JH, Lee KY, Kim MK, Shin BA, Choi SY. 2011. High cleavage efficiency of a 2A peptide derived from porcine teschovirus-1 in human cell lines, zebrafish and mice. PLoS One 6:e18556. https://doi.org/10.1371/journal.pone.0018556.
21. Gauvin L, Bennett S, Liu H, Hakimi M, Schlossmacher M, Majithia J, Brown EG. 2013. Respiratory infection of mice with mammalian reoviruses causes systemic infection with age and strain dependent pneumonia and encephalitis. Virol J 10:67. https://doi.org/10.1186/1743-422X-10-67.
22. Etoh T, Himeno Y, Matsumoto T, Aramaki M, Kawano K, Nishizono A, Kitano S. 2003. Oncolytic viral therapy for human pancreatic cancer cells by reovirus. Clin Cancer Res 9:1218–1223.
23. Hirasawa K, Nishikawa SG, Norman KL, Alain T, Kossakowska A, Lee PW. 2002. Oncolytic reovirus against ovarian and colon cancer. Cancer Res 62:1696–1701.
24. Simon EJ, Howells MA, Stuart JD, Boehme KW. 2017. Serotype-specific killing of large cell carcinoma cells by reovirus. Viruses 9:E140. https://doi.org/10.3390/v9060140..
25. Bommareddy PK, Patel A, Hossain S, Kaufman HL. 2017. Talimogene laherparepvec (T-VEC) and other oncolytic viruses for the treatment of

melanoma. Am J Clin Dermatol 18:1–15. https://doi.org/10.1007/s40257-016-0238-9.
26. Killock D. 2015. Skin cancer: T-VEC oncolytic viral therapy shows promise in melanoma. Nat Rev Clin Oncol 12:438. https://doi.org/10.1038/nrclinonc.2015.106.
27. Germain-Genevois C, Garandeau O, Couillaud F. 2016. Detection of brain tumors and systemic metastases using nanoluc and fluc for dual reporter imaging. Mol Imaging Biol 18:62–69. https://doi.org/10.1007/s11307-015-0864-2.
28. Stacer AC, Nyati S, Moudgil P, Iyengar R, Luker KE, Rehemtulla A, Luker GD. 2013. NanoLuc reporter for dual luciferase imaging in living animals. Mol Imaging 12:1–13.
29. Tran V, Moser LA, Poole DS, Mehle A. 2013. Highly sensitive real-time in vivo imaging of an influenza reporter virus reveals dynamics of replication and spread. J Virol 87:13321–13329. https://doi.org/10.1128/JVI.02381-13.
30. Boehme KW, Guglielmi KM, Dermody TS. 2009. Reovirus nonstructural protein sigma1s is required for establishment of viremia and systemic dissemination. Proc Natl Acad Sci U S A 106:19986–19991. https://doi.org/10.1073/pnas.0907412106.
31. London L, Majeski EI, Paintlia MK, Harley RA, London SD. 2002. Respiratory reovirus 1/L induction of diffuse alveolar damage: a model of acute respiratory distress syndrome. Exp Mol Pathol 72:24–36. https://doi.org/10.1006/exmp.2001.2414.
32. Haller BL, Barkon ML, Li XY, Hu WM, Wetzel JD, Dermody TS, Virgin HWT. 1995. Brain- and intestine-specific variants of reovirus serotype 3 strain dearing are selected during chronic infection of severe combined immunodeficient mice. J Virol 69:3933–3937.
33. Majeski EI, Paintlia MK, Lopez AD, Harley RA, London SD, London L. 2003. Respiratory reovirus 1/L induction of intraluminal fibrosis, a model of bronchiolitis obliterans organizing pneumonia, is dependent on T lymphocytes. Am J Pathol 163:1467–1479. https://doi.org/10.1016/S0002-9440(10)63504-3.
34. Morin MJ, Warner A, Fields BN. 1996. Reovirus infection in rat lungs as a model to study the pathogenesis of viral pneumonia. J Virol 70:541–548.
35. Hingorani P, Zhang W, Lin J, Liu L, Guha C, Kolb EA. 2011. Systemic administration of reovirus (Reolysin) inhibits growth of human sarcoma xenografts. Cancer 117:1764–1774. https://doi.org/10.1002/cncr.25741.
36. Norman KL, Coffey MC, Hirasawa K, Demetrick DJ, Nishikawa SG, DiFrancesco LM, Strong JE, Lee PW. 2002. Reovirus oncolysis of human breast cancer. Hum Gene Ther 13:641–652. https://doi.org/10.1089/10430340252837233.
37. Wilcox ME, Yang WQ, Senger D, Rewcastle NB, Morris DG, Brasher PMA, Shi ZQ, Johnston RN, Nishikawa S, Lee PWK, Forsyth PA. 2001. Reovirus as an oncolytic agent against experimental human malignant gliomas. J Natl Cancer Inst 93:903–912. https://doi.org/10.1093/jnci/93.12.903.
38. Haller BL, Barkon ML, Vogler GP, Virgin HWT. 1995. Genetic mapping of reovirus virulence and organ tropism in severe combined immunodeficient mice: organ-specific virulence genes. J Virol 69:357–364.
39. Selb B, Weber B. 1994. A study of human reovirus IgG and IgA antibodies by ELISA and Western blot. J Virol Methods 47:15–25. https://doi.org/10.1016/0166-0934(94)90062-0.
40. Tai JH, Williams JV, Edwards KM, Wright PF, Crowe JE, Jr, Dermody TS. 2005. Prevalence of reovirus-specific antibodies in young children in Nashville, Tennessee. J Infect Dis 191:1221–1224. https://doi.org/10.1086/428911.
41. Cerullo V, Pesonen S, Diaconu I, Escutenaire S, Arstila PT, Ugolini M, Nokisalmi P, Raki M, Laasonen L, Sarkioja M, Rajecki M, Kangasniemi L, Guse K, Helminen A, Ahtiainen L, Ristimaki A, Raisanen-Sokolowski A, Haavisto E, Oksanen M, Karli E, Karioja-Kallio A, Holm SL, Kouri M, Joensuu T, Kanerva A, Hemminki A. 2010. Oncolytic adenovirus coding for granulocyte macrophage colony-stimulating factor induces antitumoral immunity in cancer patients. Cancer Res 70:4297–4309. https://doi.org/10.1158/0008-5472.CAN-09-3567.
42. Yang Z, Zhang Q, Xu K, Shan J, Shen J, Liu L, Xu Y, Xia F, Bie P, Zhang X, Cui Y, Bian XW, Qian C. 2012. Combined therapy with cytokine-induced killer cells and oncolytic adenovirus expressing IL-12 induce enhanced antitumor activity in liver tumor model. PLoS One 7:e44802. https://doi.org/10.1371/journal.pone.0044802.
43. Fukuyama S, Katsura H, Zhao D, Ozawa M, Ando T, Shoemaker JE, Ishikawa I, Yamada S, Neumann G, Watanabe S, Kitano H, Kawaoka Y. 2015. Multi-spectral fluorescent reporter influenza viruses (Color-flu) as powerful tools for in vivo studies. Nat Commun 6:6600. https://doi.org/10.1038/ncomms7600.
44. Kobayashi T, Ooms LS, Ikizler M, Chappell JD, Dermody TS. 2010. An improved reverse genetics system for mammalian orthoreoviruses. Virology 398:194–200. https://doi.org/10.1016/j.virol.2009.11.037.
45. Ishii K, Ueda Y, Matsuo K, Matsuura Y, Kitamura T, Kato K, Izumi Y, Someya K, Ohsu T, Honda M, Miyamura T. 2002. Structural analysis of vaccinia virus DIs strain: application as a new replication-deficient viral vector. Virology 302:433–444. https://doi.org/10.1006/viro.2002.1622.
46. Virgin HW, Bassel-Duby R, Fields BN, Tyler KL. 1988. Antibody protects against lethal infection with the neurally spreading reovirus type 3 (Dearing). J Virol 62:4594–4604.